Biochemical and Biophysical Research Communications 395 (2010) 521–523

Contents lists available at ScienceDirect

Biochemical and Biophysical Research Communications

journal homepage: www.elsevier.com/locate/ybbrc

Raman imaging of cell wall polymers in *Arabidopsis thaliana*

Martin Schmidt [a,*], Adam M. Schwartzberg [b], Andrew Carroll [a,c], Adisorn Chaibang [d], Paul D. Adams [b], P. James Schuck [b]

[a] Energy Biosciences Institute, University of California, Berkeley, CA 94720, USA
[b] Lawrence Berkeley National Laboratory, Berkeley, CA 94720, USA
[c] Department of Biology, Stanford University, Stanford, CA 94305, USA
[d] Department of Plant & Microbial Biology, University of California, Berkeley, CA 94720, USA

ARTICLE INFO

Article history:
Received 30 March 2010
Available online 13 April 2010

Keywords:
Arabidopsis
Cell wall
Microspectroscopy
Raman imaging

ABSTRACT

We present chemical images of *Arabidopsis thaliana* stem cross-sections acquired by confocal Raman microscopy. Using green light (532 nm) from a continuous wave laser, the spatial distributions of cell wall polymers in *Arabidopsis* are visualized for the first time with lateral resolution that is sub-μm. Our results facilitate the label-free *in situ* characterization and screening of cell wall composition in this plant biology and genetics model organism, contributing ultimately towards an understanding of the molecular biology of many plant traits.

© 2010 Elsevier Inc. All rights reserved.

1. Introduction

Plant biomass constitutes a renewable energy source, which harnesses solar energy through photosynthesis, and is pivotal in providing solutions to pressing challenges facing humanity, e.g. feeding a growing global human population, mitigating global climate change, and the need of many major national economies to resort to renewable resources within the next decades. Scientific and technological advances in plant biology, genetics and biotechnology are crucial for delivering abundant renewable resources for the increased and sustainable production of food, biofuels, and chemicals. In fact, lignocellulosic biomass is poised to become the primary source of biomass for the conversion to liquid biofuels [1–4]. However, the recalcitrance of these plant cell wall materials to cost-effective and efficient degradation presents a major impediment to their use in the production of biofuels and chemicals. A detailed knowledge of the cell wall (ultra)structure and chemical composition is required to understand the specific chemical and physical obstacles to breakdown.

The model plant *Arabidopsis* provides an excellent model for probing the plant cell wall. Its small size and fast generation time allow rapid characterization of mutations and treatments. Its small genome was the first plant genome sequenced [5]. *Arabidopsis* research also benefits from a wide array of tools, including collections of gene knockouts that cover much of the genome [6] and collections of gene expression, proteomics, and gene function data [7].

Analytical chemical *in situ* methods are invaluable tools for the accurate rapid characterization of lignocellulosic materials because extractive procedures for the isolation of native components are cumbersome and inevitably destructive, bringing about significant chemical and structural modifications. Label-free chemical imaging by confocal Raman microscopy has been previously used for the *in situ* visualization of the spatial distribution of cellulose and lignin in poplar [8,9] and spruce wood [10] cell walls (i.e., non-green samples). We have recently adopted this method to compare lignification in wild type and lignin-deficient transgenic *Populus trichocarpa* (black cottonwood) stem wood [11].

Given the importance and utility of *Arabidopsis* in plant research, the application of this micro-spectroscopic analysis tool to *Arabidopsis thaliana* appears highly promising and desirable. But it has thus far been precluded by prohibitively strong autofluorescence in green samples. Here, we demonstrate high-quality Raman imaging of *A. thaliana* with visible wavelength excitation and high spatial resolution, overcoming the autofluorescence problem by using senescent samples.

2. Materials and methods

Wild type seeds of the Columbia-0 ecotype were sterilized with bleach and placed at 4 °C for 4 days. Seeds were germinated on ½ MS plates (0.5 × MS, 0.8 g/L MES, 0.7% agar, pH 5.7) and transplanted onto soil after 10 days. The stems of plants were wrapped

* Corresponding author. Address: Energy Biosciences Institute, University of California, Berkeley, 118 Calvin Laboratory, MC 5230, Berkeley, CA 94720, USA. Fax: +1 510 642 1490.
E-mail address: mwbschmidt@berkeley.edu (M. Schmidt).

0006-291X/$ - see front matter © 2010 Elsevier Inc. All rights reserved.
doi:10.1016/j.bbrc.2010.04.055

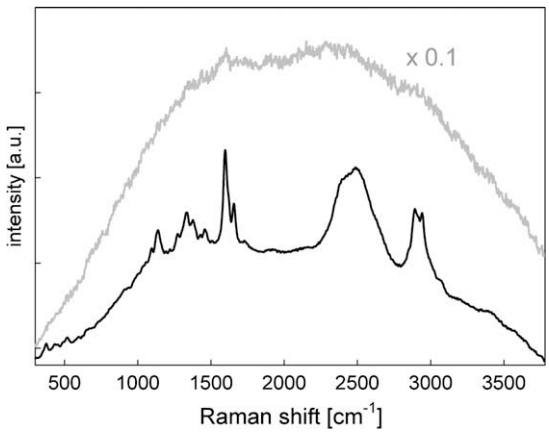

Fig. 1. Average Raman spectrum of a senescent *Arabidopsis thaliana* stem section in D_2O (black line) and a scaled Raman spectrum of a green sample with prohibitively large autofluorescence (gray line). (For interpretation of the references to color in this figure legend, the reader is referred to the web version of this paper.)

around and tied to stakes after 3 weeks, after which the plants were no longer watered. Samples were taken 3 weeks later when the stems of the plant were completely dried. About 20-μm-thick transverse sections from hydrated senescent *A. thaliana* stems were prepared by microtome (Leica, RM2265 rotary microtome). The sections were placed in D_2O (Aldrich) on glass microscope slides and covered with glass cover slips (18 × 18 × 0.17 mm). The edges of the cover slips were sealed onto the glass slides to prevent evaporation of D_2O. Two-dimensional spectral maps were acquired with a confocal Raman microscope (WITec, alpha300 S, fiber/pinhole diameter = 100 μm), which is equipped with a piezoelectric scan stage. A 100× oil immersion microscope objective (Nikon, NA = 1.40, WD = 0.13 mm) and a laser in the visible wavelength range (λ = 532 nm) were used in the measurements. The linearly polarized laser light was focused with a nearly diffraction-limited spot size onto the samples and the Raman light was detected by a CCD camera (Andor, DV401-BV) behind a grating (600 grooves mm^{-1}) spectrometer (WITec, UHTS 300) with a spectral resolution of 3 cm^{-1}. The laser power on the samples was approximately 6 mW. The lateral resolution of our system was determined via a knife-edge measurement within our sample fluid cell to be ~300 nm, which is near the theoretical limit ($0.61\lambda/NA \approx 230$ nm). Sample areas of interest were mapped by raster scanning in 200-nm steps with an integration time of 100 ms per spectrum. The WITec Project software (version 1.94) was used for spectral and image processing and analysis. Chemical images were computed from the two-dimensional spectral maps by integrating the intensity over a defined wavenumber range in the baseline-corrected Raman spectra.

3. Results

Fig. 1 shows an average Raman spectrum of a senescent *A. thaliana* xylem section in D_2O. The Raman bands are attributable primarily to the major cell wall polymers, i.e., cellulose, hemicelluloses, and lignin as well as D_2O. Band assignments are given in the literature [8–12]. For comparison, a scaled Raman spectrum of a green sample is also presented. Apart from the large fluorescence background it is virtually featureless, rendering such a green sample unsuitable for Raman analysis.

To obtain chemical images, position-resolved micro-spectroscopic measurements were performed acquiring two-dimensional spectral maps. The basic morphology of the measured cell walls becomes apparent in the chemical image based on the composite C–H stretching bands, i.e., integrating the intensity over the range from 2775 to 3125 cm^{-1} (Fig. 2A). The spatial distribution of the carbohydrates, mainly cellulose, is visualized by integrating the intensity from 2820 to 2935 cm^{-1} (Fig. 2B) [9]. As expected, high carbohydrate signals are found in the secondary walls. In Fig. 2C the lignin distribution is presented, obtained by integrating from 1550 to 1700 cm^{-1} [8–11]. High lignin signal intensity is observed

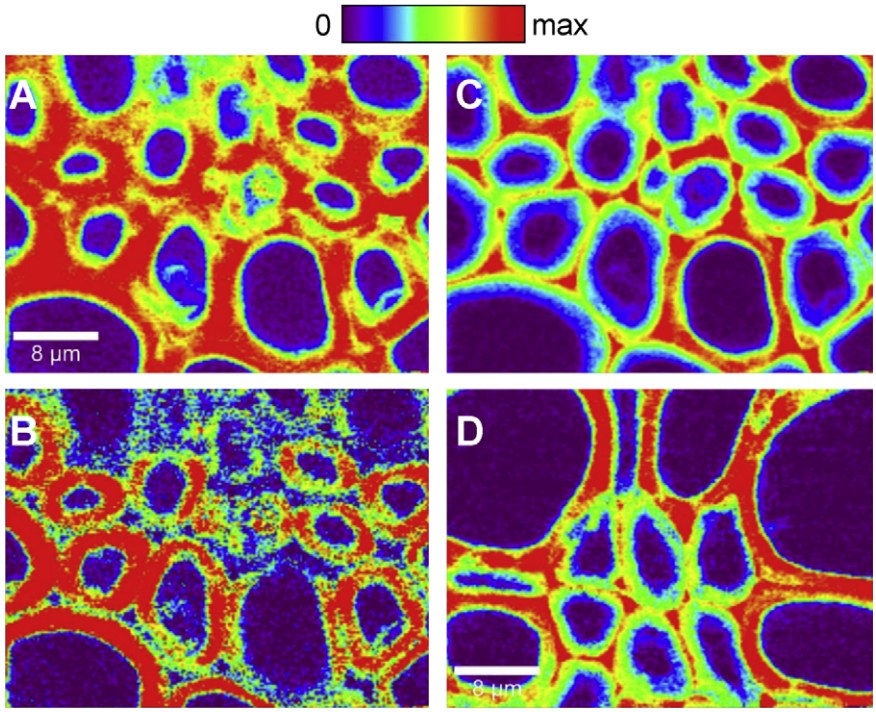

Fig. 2. Chemical images of a xylem tissue cross-section of senescent *Arabidopsis thaliana* based on: (A) the composite C–H stretching bands (integrating the intensity from 2775 to 3125 cm^{-1}), (B) the C–H and CH_2 stretching of carbohydrates (2820–2935 cm^{-1}), and (C) lignin Raman bands (1550–1700 cm^{-1}). (D) Variability in the spatial distribution of the lignin signal intensity.

in the cell corners and, somewhat less, in the compound middle lamellae. For many cells lower, yet not insubstantial, amounts of lignin are observed within the secondary walls. However, there is variability of the lignin signal intensity and some secondary walls, namely of xylem vessels, are strongly lignified (Fig. 2D). This stronger lignification is likely to ensure waterproofing of these water-carrying structures.

4. Discussion

Lignocellulosic materials are hierarchical and heterogeneous with regard to both structure and composition. As shown, Raman imaging gives insights into cell wall composition with spatial resolution that is sub-μm without staining or labeling of the samples in a close to native state. It requires minimal sample preparation and the measurements are non-destructive and comparatively inexpensive. The Raman spectra register simultaneously contributions of active vibrations from all components in the sample volume. To fully exploit the multicomponent and multiphase sensitivity, i.e., the multiplex advantage, we are currently pursuing a chemometric approach to dissect the spatial distribution of the carbohydrates, which bear structural and spectral similarities. Measuring in D_2O enables us to perform intensity normalization based on the extrinsic O–D stretching band around 2500 cm^{-1} in the average lumen spectra [11]. This is critical and allows us to compare signal intensities between different measurements, tissues, samples and species.

5. Conclusion

Using senescent samples, Raman imaging of cell wall polymers in *A. thaliana* was demonstrated. The spectral analysis is not limited to cellulose and lignin, and a chemometric approach can make hemicelluloses and pectin accessible [13]. Our results facilitate the label-free *in situ* characterization and screening of different tissues and mutants. Mutations can be correlated with variations in cell wall composition and structure relatively fast and inexpensively [11]. This may ultimately contribute towards an understanding of the molecular biology of many plant traits.

Acknowledgments

This work was supported by the Energy Biosciences Institute and the US Department of Energy (Grant DOE-FG02-03ER20133). Work at the Molecular Foundry was supported by the Office of Science, Office of Basic Energy Sciences, of the US Department of Energy under Contract No. DE-AC02-05CH1123.

References

[1] S. Herrera, Bonkers about biofuels, Nat. Biotechnol. 24 (2006) 755–760.
[2] A.J. Ragauskas, C.K. Williams, B.H. Davison, G. Britovsek, J. Cairney, C.A. Eckert, W.J. Frederick, J.P. Hallett, D.J. Leak, C.L. Liotta, J.R. Mielenz, R. Murphy, R. Templer, T. Tschaplinski, The path forward for biofuels and biomaterials, Science 311 (2006) 484–489.
[3] M.E. Himmel, S.Y. Ding, D.K. Johnson, W.S. Adney, M.R. Nimlos, J.W. Brady, T.D. Foust, Biomass recalcitrance: engineering plants and enzymes for biofuels production, Science 315 (2007) 804–807.
[4] A. Carroll, C. Somerville, Cellulosic biofuels, Annu. Rev. Plant Biol. 60 (2009) 165–182.
[5] S. Kaul, H.L. Koo, J. Jenkins, M. Rizzo, T. Rooney, L.J. Tallon, T. Feldblyum, W. Nierman, M.I. Benito, X.Y. Lin, C.D. Town, J.C. Venter, C.M. Fraser, S. Tabata, Y. Nakamura, T. Kaneko, S. Sato, E. Asamizu, T. Kato, H. Kotani, S. Sasamoto, J.R. Ecker, A. Theologis, N.A. Federspiel, C.J. Palm, B.I. Osborne, P. Shinn, A.B. Conway, V.S. Vysotskaia, K. Dewar, L. Conn, C.A. Lenz, C.J. Kim, N.F. Hansen, S.X. Liu, E. Buehler, H. Altafi, H. Sakano, P. Dunn, B. Lam, P.K. Pham, Q. Chao, M. Nguyen, G.X. Yu, H.M. Chen, A. Southwick, J.M. Lee, M. Miranda, M.J. Toriumi, R.W. Davis, R. Wambutt, G. Murphy, A. Dusterhoft, W. Stiekema, T. Pohl, K.D. Entian, N. Terryn, G. Volckaert, M. Salanoubat, N. Choisne, M. Rieger, W. Ansorge, M. Unseld, B. Fartmann, G. Valle, F. Artiguenave, J. Weissenbach, F. Quetier, R.K. Wilson, M. de la Bastide, M. Sekhon, E. Huang, L. Spiegel, L. Gnoj, K. Pepin, J. Murray, D. Johnson, K. Habermann, N. Dedhia, L. Parnell, R. Preston, L. Hillier, E. Chen, M. Marra, R. Mart. ienssen, W.R. McCombie, K. Mayer, O. White, M. Bevan, K. Lemcke, T.H. Creasy, C. Bielke, B. Haas, D. Haase, R. Maiti, S. Rudd, J. Peterson, H. Schoof, D. Frishman, B. Morgenstern et al., Analysis of the genome sequence of the flowering plant *Arabidopsis thaliana*, Nature 408 (2000) 796–815.
[6] J.M. Alonso, A.N. Stepanova, T.J. Leisse, C.J. Kim, H. Chen, P. Shinn, D.K. Stevenson, J. Zimmerman, P. Barajas, R. Cheuk, C. Gadrinab, C. Heller, A. Jeske, E. Koesema, C.C. Meyers, H. Parker, L. Prednis, Y. Ansari, N. Choy, H. Deen, M. Geralt, N. Hazari, E. Hom, M. Karnes, C. Mulholland, R. Ndubaku, I. Schmidt, P. Guzman, L. Aguilar-Henonin, M. Schmid, D. Weigel, D.E. Carter, T. Marchand, E. Risseeuw, D. Brogden, A. Zeko, W.L. Crosby, C.C. Berry, J.R. Ecker, Genome-wide insertional mutagenesis of *Arabidopsis thaliana*, Science 301 (2003) 653–657.
[7] S.Y. Rhee, W. Beavis, T.Z. Berardini, G.H. Chen, D. Dixon, A. Doyle, M. Garcia-Hernandez, E. Huala, G. Lander, M. Montoya, N. Miller, L.A. Mueller, S. Mundodi, L. Reiser, J. Tacklind, D.C. Weems, Y.H. Wu, I. Xu, D. Yoo, J. Yoon, P.F. Zhang, The *Arabidopsis* Information Resource (TAIR): a model organism database providing a centralized, curated gateway to *Arabidopsis* biology, research materials and community, Nucleic Acids Res. 31 (2003) 224–228.
[8] N. Gierlinger, M. Schwanninger, Chemical imaging of poplar wood cell walls by confocal Raman microscopy, Plant Physiol. 140 (2006) 1246–1254.
[9] N. Gierlinger, I. Burgert, Secondary cell wall polymers studied by confocal Raman microscopy: spatial, distribution, orientation, and molecular deformation, N. Z. J. For. Sci. 36 (2006) 60–71.
[10] U.P. Agarwal, Raman imaging to investigate ultrastructure and composition of plant cell walls: distribution of lignin and cellulose in black spruce wood (*Picea mariana*), Planta 224 (2006) 1141–1153.
[11] M. Schmidt, A.M. Schwartzberg, P.N. Perera, A. Weber-Bargioni, A. Carroll, P. Sarkar, E. Bosneaga, J.J. Urban, J. Song, M.Y. Balakshin, E.A. Capanema, M. Auer, P.D. Adams, V.L. Chiang, P.J. Schuck, Label-free *in situ* imaging of lignification in the cell wall of low lignin transgenic *Populus trichocarpa*, Planta 230 (2009) 589–597.
[12] D.S. Himmelsbach, S. Khahili, D.E. Akin, Near-infrared-Fourier-transform-Raman microspectroscopic imaging of flax stems, Vib. Spectrosc. 19 (1999) 361–367.
[13] N. Gierlinger, L. Sapei, O. Paris, Insights into the chemical composition of *Equisetum hyemale* by high resolution Raman imaging, Planta 227 (2008) 969–980.